

Cite this: *J. Mater. Chem. C*, 2013, **1**, 4138

Organic microbelt array based on hydrogen-bond architecture showing polarized fluorescence and two-photon emission†

Dongpeng Yan,^{*a} William Jones,^b Guoling Fan,^a Min Wei^a and David G. Evans^a

While organic micro/nanostructures for optoelectronic applications have attracted increasing recent attention, the assembly of aligned micro/nanostructure arrays continues to be a challenge. Herein, a one-dimensional (1D) microbelt has been fabricated by a hydrogen bonding assembly strategy with guanidinium cations and stilbene-based sulfonate anions as the building blocks. X-ray diffraction and high-resolution transmission electron microscopy demonstrate that the microbelt possesses a periodic layered structure with guanidinium cations and anionic stilbene-based chromophores regularly assembled within the microcrystal. The individual 1D microbelts show enhanced luminescent properties compared with pure stilbene-based units, with strong blue emission with a photoluminescent quantum yield of 46% and fluorescence lifetime of 2.8 ns, as well as well-defined polarized luminescence (an anisotropy value of 0.71). Moreover, a macroscopic 1D microbelt array can be fabricated by means of the spontaneous alignment of individual microbelts resulting from an evaporation-induced deposition process. The regularly oriented microbelt array maintains a uniform and highly polarized fluorescence and also exhibits both strong two-photon emission and an interesting second-harmonic response upon excitation with near-infrared laser pulses. Therefore, this work provides a procedure for the facile bottom-up self-assembly of highly ordered 1D organic microcrystal and microarray structures with high luminescent efficiency as well as polarized emission, which have potential applications in the areas of light displays, polarized thin films, frequency doubling materials and miniaturized optoelectronic devices.

Received 20th March 2013
Accepted 25th April 2013

DOI: 10.1039/c3tc30523f

www.rsc.org/MaterialsC

1 Introduction

Organic chromophores with one-dimensional (1D) micro/nanostructures¹ have received much attention recently due to their unique optical properties as well as promising optoelectronic applications in the fields of lasers,² waveguides,³ chemical sensors,⁴ polarized luminescence⁵ and semiconductor devices.⁶ Compared with the inorganic counterpart, the organic chromophore materials usually involve simple processing, easily tunable structure, as well as facilitating the fabrication of flexible and soft optical devices.^{6c} However, in contrast to the case of inorganic micro/nanomaterials with controllable morphologies and tunable properties,⁷ obtaining a satisfactory

performance from such 1D organic micro/nanostructures continues to be a major goal.⁸ For example, organic π -conjugated systems usually exhibit low efficiencies of light emission on formation into solid-state 1D micro/nanostructures because of strong intermolecular π - π stacking interactions resulting in the concentration quenching of luminescence,⁹ which restricts the use of these materials in solid-state optical devices. To date, examples of organic micro/nanomaterials with high emission are still limited.¹⁰ Moreover, in terms of both fundamental studies and practical applications, the ability to modulate and control the orientation of the 1D micro/nanomaterials is of critical importance for the construction of next-generation miniaturized optoelectronic devices;¹¹ although highly oriented inorganic micro/nanostructures¹² such as InGaN have been developed during last few decades, to obtain such well-arranged 1D organic micro/nanoarrays for certain photofunctional applications remains, however, a challenge.¹³

Recent advances in supramolecular chemistry have shed light on the assembly of 1D micro/nanostructured crystalline solids based on the molecular recognition between low-molecular-weight building blocks.¹⁴ Such bottom-up self-assembly offers new opportunities to solve the problem of self-quenching in the solid state for organic micro/nanomaterials

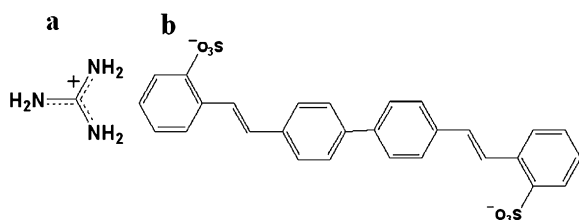
^aState Key Laboratory of Chemical Resource Engineering, Beijing University of Chemical Technology, Beijing, 100029, P. R. China. E-mail: yandp@mail.buct.edu.cn; yandongpeng001@163.com; Fax: +86-10-64425385; Tel: +86-1064412131

^bDepartment of Chemistry, University of Cambridge, Lensfield Road, Cambridge, CB2 1EW, UK

† Electronic supporting information available: SEM profiles for the GD₂BSB microbelt (Fig. S1); photoluminescence (PL) spectrum of the pristine BSB sample (Fig. S2); PL spectrum of the GD₂BSB microbelt sample excited by 800 nm with a xenon lamp (Fig. S3); PL spectrum of the pristine BSB sample excited by a 800 nm laser (Fig. S4). See DOI: 10.1039/c3tc30523f

due to the highly flexible tunability and controllability of weak non-covalent interactions.¹⁵ Hydrogen bonding (H-bonding) is a type of non-covalent interaction frequently used in the design of organic solid materials,¹⁶ and has been demonstrated as a potential tool to build functional micro/nanostructures.¹⁷ To obtain organic micro/nanomaterials with the desired morphology and function, rational selection and fine tuning of the geometrical matching and directionality of the H-bonding components play a key role.¹⁸ The guanidinium cation is a well-known H-bonding motif, which has been successfully assembled with sulfonate-bearing anions for engineering bulk crystal topologies.¹⁹ However, few guanidinium sulfonate systems have been observed in micro/nanostructured crystals and their exact properties at the micro/nanometer scale are still unknown.

Stilbene and its derivatives are of growing interest as luminescent materials because of their excellent optical and electronic properties.²⁰ The groups of Tang,^{10a,c,20f} Hadziioannou,^{20c,d} Park,^{1c,11c,20f} and Weder^{11e,20a,b} have done important work in the stilbene-based materials. However, to the best of our knowledge, there have been few examples of the tuning of the optical properties of orderly micro/nanostructures based on stilbene. In this work, we have taken advantage of the strong H-bonding recognition strategy to fabricate 1D organic microbelts with a 2D layered structure using the guanidinium cation $[C(NH_2)_3]^+$ (Scheme 1a) and an anionic sulfonated stilbene derivative, 4,4'-bis(2-sulfonatostyryl)biphenyl (BSB, Scheme 1b) as the basic building blocks. The as-prepared microbelts show well-defined blue-light emission as well as enhanced photoluminescence quantum yield and fluorescence lifetime compared with the pure BSB molecules. In addition, the presence of well-ordered organic chromophores within the microstructure also endows it with highly polarized fluorescence. Moreover, a microbelt array regularly aligned in parallel with a substrate has been obtained on the millimeter scale by an evaporation-induced deposition process.^{6a,21} The resulting microbelt array retains polarized fluorescence and shows an interesting two-photon fluorescence and nonlinear optical response. The strategy described here for the design and assembly of 1D microstructures based on H-bonding interactions allows the fabrication of orientational array material with potential future applications in optical and optoelectronic devices at the micro/nanometer level with integrated functions, such as polarized emission, two-photon luminescence and nonlinear optical behavior.



Scheme 1 Chemical structures of (a) guanidinium cation (GD) and (b) 4,4'-bis(2-sulfonatostyryl) biphenyl (BSB).

2 Results and discussion

2.1 Morphology and structure

Fig. 1a shows a typical scanning electron microscopy (SEM) image of the 1D micro/nanostructures obtained after hydrothermal treatment for 8 hours, from which it can be observed that the two ends of the micro/nanostructure had a needle-like morphology, suggesting that the growth of the crystal nucleus began from the centre of the micro/nanostructure and continued to the ends. At high concentration, the assembled materials tended to form bundles of aligned micro/nanostructures (inset in Fig. 1a). However micro/nanostructures with high monodispersity were obtained by diluting the as-prepared sample as shown in Fig. 1b. The products are 1D microbelts, and each individual microstructure has a smooth surface and a uniform length of *ca.* 30 μm . These microbelts exhibit well-resolved blue emission under UV irradiation (inset in Fig. 1b). The diameter at the centre of the microbelts can be estimated to be *ca.* 1 μm , as shown in both SEM (Fig. 1c) and transmission electron microscopy (TEM, Fig. 1d) images. The growth of the microstructure can be controlled by tuning the preparation conditions in the hydrothermal reaction. For example, the length of the microbelts can be readily increased to more than 100 μm under hydrothermal conditions by increasing the reaction time for 24 h as shown in Fig. S1 in the ESI.† Fig. 1e shows a typical high-resolution TEM (HRTEM) image of a single microbelt, in which well-defined crystal planes with a lattice distance of ~ 1.5 nm can be resolved along the long-axis direction of the microbelt, suggesting a high degree of molecular orientation within the microcrystal. Elemental analysis shows that the ratio of GD to BSB in obtained microbelts is *ca.* 2.05, approximately close to that of the idealized components (2 : 1).

The powder X-ray diffraction (XRD) pattern of the GD₂BSB microbelts is shown in Fig. 2a. The main reflections of the microbelt can be indexed to the basal spacing d_{001} (1.59 nm) and the corresponding second-order reflection d_{002} (0.80 nm) of a layered structure. The basal spacing is similar to the lattice spacing along the long-axis direction of the microbelt observed by HRTEM (Fig. 1e), indicating that the long-axis direction of the microbelt is the (00*l*) direction. The presence of a layered stacking structure with a periodicity of 1.59 nm arising from a strong H-bonding assembly (N–H \cdots O=S) between the GD and BSB units, is consistent with the structural model shown in the inset of Fig. 2a. The strong 00*l* diffraction peaks are indicative of the highly crystalline structure of the microbelts. Considering both the BSB and GD have highly symmetric structures, Raman spectroscopy was employed to characterize the molecular vibrations within the microbelt and the pristine BSB. The Raman bands are assigned based on the literature.²² For the pristine BSB sample (Fig. 2bA), the characteristic stretching vibration bands of C=C in phenylenevinylene appear at 1629, 1600, 1450 and 1330 cm^{-1} , and the peaks located at 1284 and 1187 cm^{-1} can be assigned to the symmetric and asymmetric vibration bands of S=O in the sulfonate group. Upon assembly with the GD to form the GD₂BSB microbelts (Fig. 2bB), no obvious change appeared in the C=C vibration bands of the phenylenevinylene group, while the vibration bands of S=O

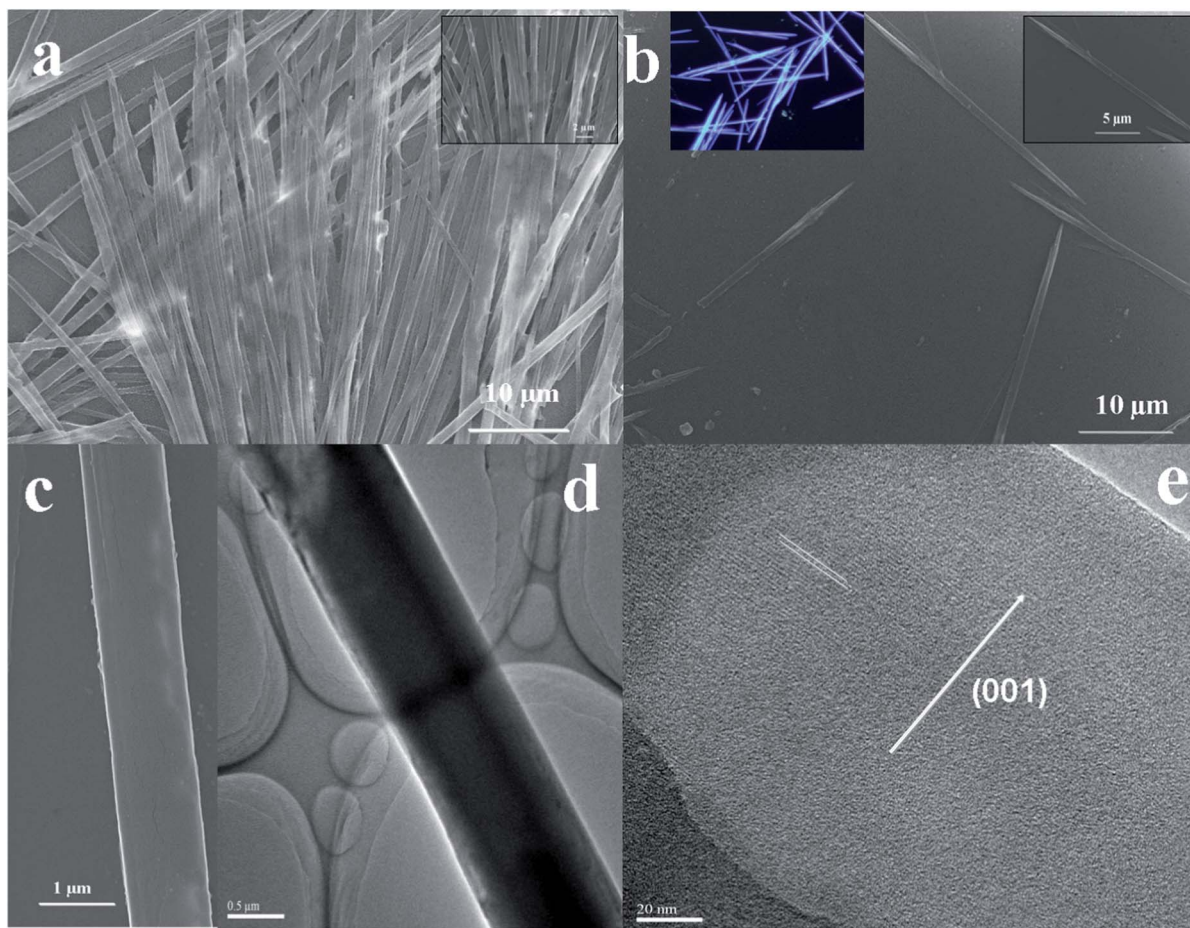


Fig. 1 (a) and (b) SEM profiles for the GD₂BSB microbelt (the left inset in b) shows GD₂BSB under 365 nm UV irradiation; (c) the single GD₂BSB microbelt; (d) TEM and (e) HRTEM images of a single GD₂BSB microbelt.

experienced a high-frequency shift and were located at 1196 cm^{-1} ($\Delta = 12\text{ cm}^{-1}$) and 1284 cm^{-1} ($\Delta = 4\text{ cm}^{-1}$), indicative of a strong H-bonding interaction between the sulfonate and N-H groups. Furthermore, the C=N vibration in GD can also be observed at *ca.* 1408 cm^{-1} . The high intensity of the Raman scattering of the C=C vibration bands also suggests the presence of high polarizability within the 1D micro/nanostructures.

2.2 Photophysical properties

Fig. 3a shows the typical fluorescence spectra of the microbelt sample, in which the excitation and emission peaks are located at 281 and 448 nm respectively. Compared with the pure BSB powder sample which has an emission peak at 463 nm and a shoulder band at 487 nm related to chromophore aggregation/excimer (ESI: Fig. S2[†]), the as-prepared microbelt exhibits a blue-shifted emission of *ca.* 15 nm ($6.7 \times 10^5\text{ cm}^{-1}$). Such a blue-shift in the spectrum of the microbelt samples may be assigned to the size- and shape-dependent effect, since it is well documented that the size of micro/nanomaterial particles has a strong correlation with their optical properties.^{3c,13b} In addition, the alternation of the molecular arrangements and different degrees of self-absorption may also contribute to different

emission maxima.^{20m} Moreover, the as-prepared GD₂BSB microstructure exhibited an absolute photoluminescent quantum yield (PLQY) of 46%, which is significantly higher than the value for pure BSB (18%), and also higher than the reported values for most organic solid-state chromophores.^{20g} Such a remarkable enhancement of the light-emission efficiency can be attributed to the high degree of organization of BSB molecules within the highly crystalline microstructure owing to the strong H-bonding interactions, which restricts the thermal vibration and configuration relaxation. Moreover, the GD units within the microcrystal can isolate the BSB anions from each other, and thus molecular aggregation can be eliminated. This is confirmed by the absence from the emission spectrum of GD₂BSB of the shoulder band observed at long wavelength in the spectrum of pure BSB. To further investigate the nature of the excited states, the fluorescence lifetimes of the microbelt sample were recorded. Fig. 3b shows a comparison of the typical fluorescence decay curves of powdered and dilute aqueous solutions of BSB with that for the GD₂BSB microbelts. The fluorescence lifetimes of both the BSB solution and powdered samples are 1.8 ns, while that of the GD₂BSB microbelts is 2.8 ns. The increased excited-state fluorescence lifetime upon introduction of the GD building blocks confirms

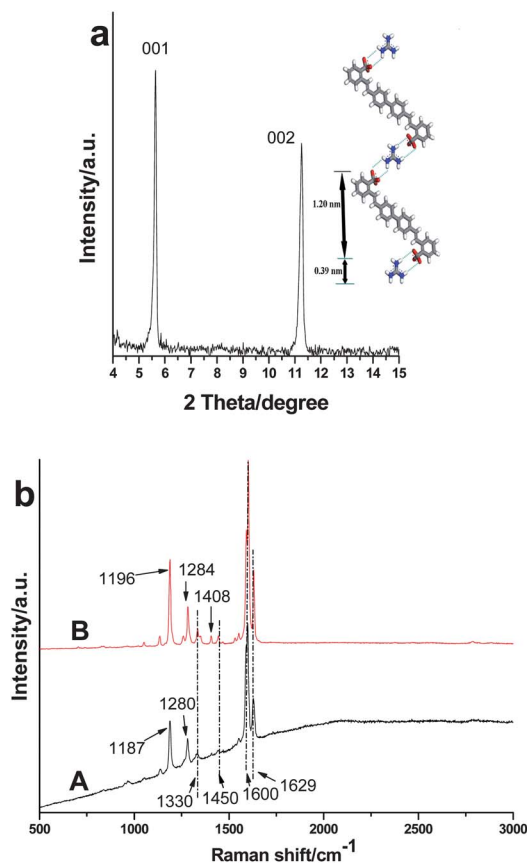


Fig. 2 (a) Powder XRD patterns of GD₂BSB; (b) Raman spectra of the (A) pristine BSB and (B) GD₂BSB microbelt.

that the formation of H-bonding assembled microstructures can effectively suppress the nonradiative fluorescence decay of the BSB anions.^{20k,l} Therefore, the introduction of the H-bonding units within the crystalline chromophore based on supramolecular architecture may pave a way to solve the problem of the low-efficiency fluorescence of organic materials in the solid state.

2.3 Fluorescence microscopy of the microbelts

Under a fluorescence microscope, the blue emission of a single microbelt can be easily imaged due to its high PLQY. The power-dependent emission spectrum of a single microbelt was measured and compared with that of the bulk. Upon laser excitation at 405 nm, the single microbelt showed increasing fluorescence intensity with increasing excitation intensity as shown in Fig. 4a. The main emission peak of the single microbelt appeared at *ca.* 450 nm, and no obvious shift in the emission maximum of the individual microbelt was observed compared to the microbelt ensemble. In addition, the dark-field images of the selected microbelt excited with different laser power (5 mW and 30 mW) are visible to the naked eye as shown in the inset of Fig. 4a. When the single microbelt crystal was excited with the excitation light polarized parallel to its long-axis direction, the emission intensities varied significantly between the parallel (I_{\parallel}) and perpendicular (I_{\perp}) polarized

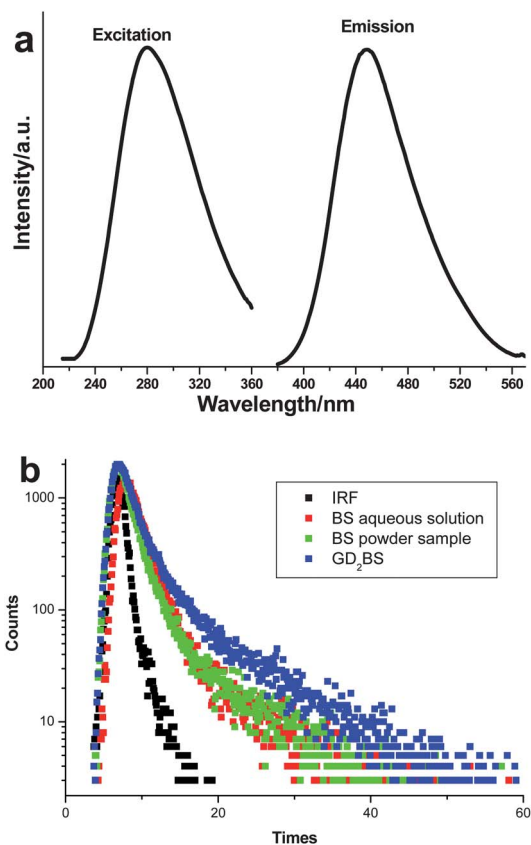


Fig. 3 (a) Fluorescence spectra of the GD₂BSB microbelts (excitation wavelength: 290 nm, emission wavelength: 448 nm); (b) the fluorescence decay curves of the powdered and pure dilute aqueous solution of BSB as well as the GD₂BSB microbelts (IRF denotes the instrument response function).

directions, with an anisotropy value²⁴ r ($r = (I_{\parallel} - I_{\perp}) / (I_{\parallel} + 2I_{\perp})$) of 0.71. The strongly polarized emission of the single microbelt can be observed directly, as shown in the inset of Fig. 4b.

The high degree of fluorescence polarization can be attributed to the high degree of organization and high anisotropy of the BSB molecular packing within the 1D microcrystal, as illustrated by XRD and TEM (see above). The microbelt exhibits its highest emission intensity when the direction of polarization is parallel with the transition dipole moment of BSB molecules. The presence of polarized fluorescence can be further confirmed by the observation of two microbelts perpendicular to each other, which exhibit alternate bright and dark emission upon rotating the polarizer by 90° (shown in Fig. 4c).

2.4 Characterization of microbelt array

The presence of polarized fluorescence means that if the microbelts are arranged at random within a film this cannot result in a well-defined macroscopic polarization. Therefore if the luminescent microbelts are to be used in photofunctional devices, such as the background illumination source of a liquid crystal display, they must first be formed into an ordered array. Moreover, in a film for use in optoelectronic devices with polarized emission, the microbelts should be oriented parallel, rather than perpendicular, to the substrate.²³

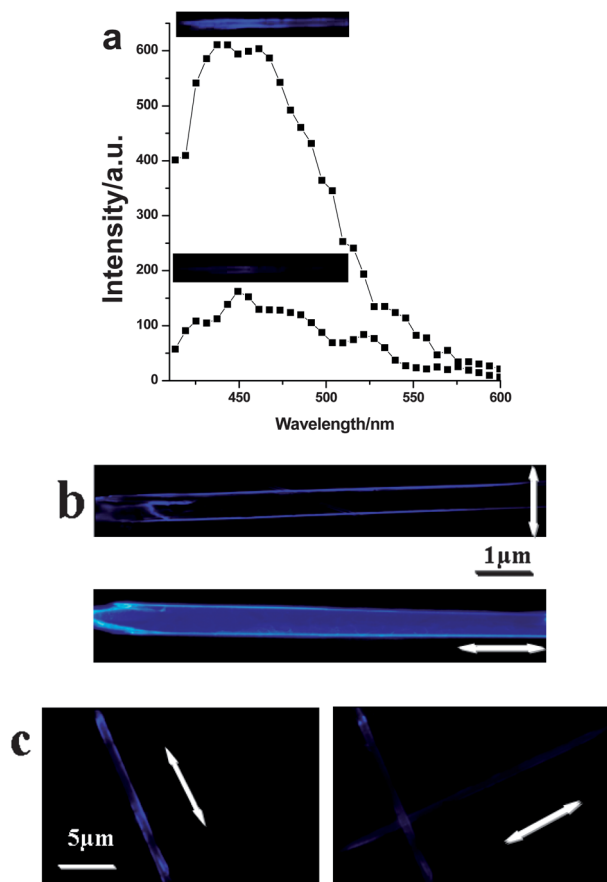


Fig. 4 (a) Fluorescence spectra and corresponding microscope images (inset plots) for an individual microbelt excited by a laser (5 mW and 30 mW) at 405 nm; (b) and (c) fluorescence microscope images for one single and two perpendicular microbelts under UV irradiation (365 nm) in different polarization directions.

Thus patterning the micro/nanostructures is important for rational design of a low-dimensional micro/nanodevice for optical application. To the best of our knowledge, organic patterned micro/nano-structural film with high orientation have attracted limited attention^{11e,f} than those of inorganic materials. Here we use an evaporation-induced deposition process^{6a,21} to form a well-defined microbelt array on a glass substrate. Fig. 5a shows the resulting aligned 1D microstructures having nearly the same length over a macroscopic area under a fluorescence microscope, in which the microbelts exhibit a regular arrangement with a gap of *ca.* 100 μm between each row of microstructures. This observation confirms the self-organization of the individual 1D microstructure into an array structure during the evaporation process. In addition, the needle-like tips of the microstructures may also facilitate the formation of a regular pattern during the evaporation of solvent, in which the surface tension can further modulate and adjust the microstructure in a same direction upon water evaporation. Thus, the method offers a facile bottom-up way to pattern a microbelt array without the necessity for manipulation by lithography or other external forces.^{8b,11c,27} An expanded fluorescence

microscope image (Fig. 5b) confirms that the microbelts have almost the same size and shape, and are nearly parallel to each other in the microbelt array, which results in relatively uniform blue emission by detecting the emission intensity dependent on the direction vertical to the long-axis of microbelts (Fig. 5c). Fig. 5d shows a selected region which exhibits homogeneously bright emission under unpolarized excitation. Upon excitation by UV polarized light at 365 nm, the microbelt array exhibit well-defined polarized luminescence between the directions parallel and perpendicular to the long-axis direction as shown in Fig. 5e and f. The typical polarized emission profile is shown in Fig. 5g, and the anisotropy value r at 450 nm is *ca.* 0.49, which is smaller by 44% than that for a single microbelt. This difference can be attributed to the less than perfect ordering of the microbelts on the substrate. In addition, the anisotropy value is comparable with other reported 1D nanofibers^{17b} and some conjugated polymer film systems,²² although this is still low for targeted application in displays.

Encouraged by the high polarizability observed by Raman spectroscopy and the polarized emission study as well as the up-conversion phenomenon of the stilbene component, two-photon excited fluorescence measurements were then made. Upon irradiation by a femtosecond pulsed laser at 800 nm, the GD₂BSB microbelt array exhibited strong two-photon fluorescence with a maximum emission peak at *ca.* 450 nm (Fig. 6), which can be further visualized in the inset in Fig. 6. The emission peaks had no obvious red- or blue-shift compared with those excited by UV light, demonstrating that emission processes from both one-photon and two-photon excited states to the ground state are involved. Moreover, the emission intensity showed a nearly quadratic increase as a function of the incident energy, showing that the up-converted emission is derived from a two-photon-absorption mechanism. In addition, the two-photon emission of the microbelt array could even be obtained with a xenon lamp as excitation source on a standard spectrofluorimeter as shown in Fig. S3 in the ESI.† More interestingly, a strong second-harmonic laser emission at 400 nm from the microbelt array was also observed, with the intensity also showing a square dependence on the incident energy. Such a second-order nonlinear optical effect can be attributed to the high polarizability of the GD₂BSB microbelts as well as their regular non-centrosymmetric orientation within the 1D microcrystal array. In contrast, the pure BSB disodium salt had no such response under the same conditions as shown in Fig. S4 in the ESI.† To the best of our knowledge, although nonlinear optical effects have been widely reported for both inorganic and organic macroscopic crystal systems,²⁵ few of such an effect has been observed in a 1D microcrystal array system. As a result, the solid-state samples can serve as two-photon fluorescence and nonlinear optical materials. The two-photon emission and second harmonic generation that convert the near-infrared light (800 nm) to both the visible (410–550 nm) and UV light (400 nm) further illustrate such a 1D microcrystal array system may be potentially applied in frequency doubling,²⁶ nonlinear optics and up-conversion lasers.

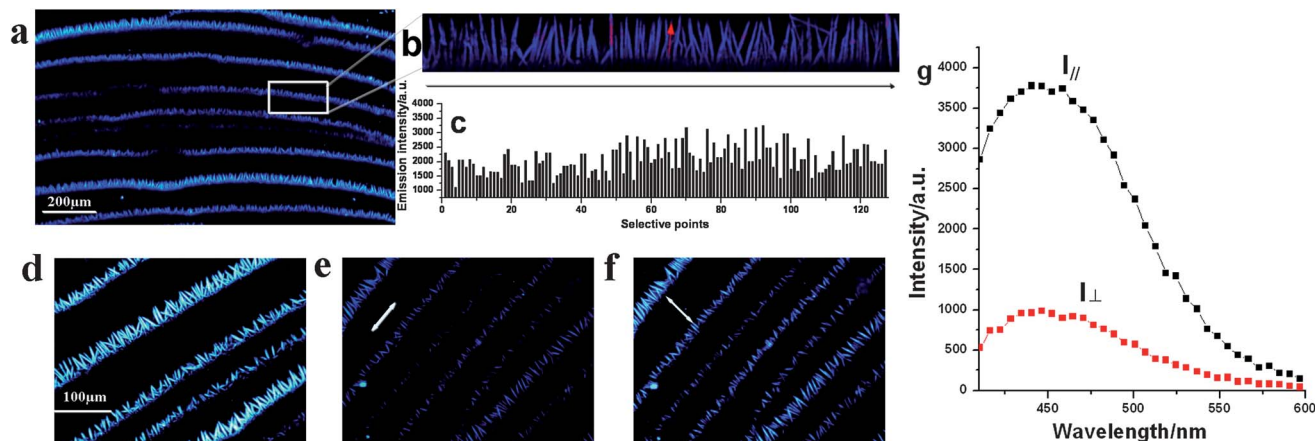


Fig. 5 (a) and (b) Fluorescence microscope images of a GD₂BSB microbelt array with different magnifications. (c) The relative emission intensity for the microbelt array within the selected points in the region shown in (b). Fluorescence microscope images of the microbelt array with (d) unpolarized emission, (e) polarized emission perpendicular to and (f) parallel to the direction of the long-axis of the microbelt. (g) Typical polarized fluorescence spectra for (e) and (f).

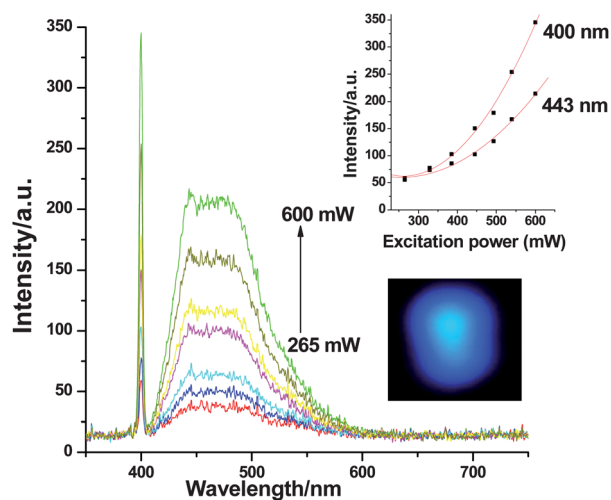


Fig. 6 Two-photon fluorescence spectra of the GD₂BSB microbelt excited by 800 nm femtosecond laser pulses with different pumping intensities. The inset plot shows the changes in intensity at 400 and 443 nm with increasing pumping intensity. The inset image shows a photograph of the microbelt array under irradiation by a 800 nm laser.

3 Conclusion

Fluorescent microbelts have successfully been fabricated using a combination of co-precipitation and a hydrothermal method based on a strong H-bonding assembly strategy. The as-prepared GD₂BSB microbelts exhibit superior luminescence performance (such as enhanced PLQY and fluorescence lifetime as well as high fluorescence polarization) compared to the pure BSB building blocks, due to the highly crystalline nature and ordered assembly of the ions within the crystal. Moreover, the well-organized 1D microbelt array was also assembled into a film using an evaporation-induced deposition process. The macroscopic scale patterned film shows homogeneously polarized fluorescence (with an anisotropy value $r = 0.49$) with tunable emissive intensity in different polarization directions.

In addition, the microbelt array exhibits both two-photon emission and an interesting second harmonic generation upon excitation with femtosecond near-infrared light pulses, making it a potential candidate for applications in the optoelectronic field, such as micro/nanolasers, up-conversion optical devices and polarized emission materials.

4 Experimental

4.1 Reagents and materials

Guanidinium chloride (GD) and disodium 4,4'-bis (2-sulfonastoyryl)biphenyl (BSB) were purchased from Sigma Chemical Co., Ltd. and used without further purification.

4.2 Fabrication of GD₂BSB microbelts and array structures

The microbelts were obtained by a combined co-precipitation and sonochemistry method, followed by hydrothermal treatment. In a typical process, a 30 mL of an aqueous solution containing 0.002 mol of GD (solution A) and a 30 mL of an aqueous solution containing 0.001 mol of BSB (solution B) were simultaneously added to a container under low-intensity ultrasonic radiation (using an ultrasonic cleaning bath with a frequency of 25 kHz), and mixed for 3 min. The resulting slurry was removed and sealed into a 90 mL Teflon-lined stainless steel autoclave, and heated at 100 °C for 8–24 hours. The product was washed several times with distilled water until the washings showed no fluorescence. The resulting solid remained well-dispersed in water for an extended period of time. Elemental analysis gave C 50.4%, H 4.6%, N 23.6%, S 8.8%, so the chemical composition of microbelt can be determined as: (C₂N₆H₆)_{2.05}(C₂₈H₂₀S₂O₆). The GD₂BSB microbelt array was obtained by the evaporation-induced deposition method. Typically, a glass or quartz substrate was vertically dipped into the solution containing well-dispersed GD₂BSB microbelts for 2 min, and then slowly removed from the solution and allowed to dry naturally under ambient conditions.

4.3 Characterization

Powder X-ray diffraction (XRD) patterns were recorded on a Rigaku D/MAX2500VB2+/PC X-ray diffractometer, using Cu K α radiation (0.154184 nm) at 40 kV, 30 mA with a scanning rate of 5° min⁻¹, a step size of 0.02° s⁻¹, and a 2 θ angle ranging from 3 to 20°. Raman spectra were recorded using an inVia Reflex Raman spectrometer in the range 3000–500 cm⁻¹ with 2 cm⁻¹ resolution in air. C, H, N, and S analyses were carried out using a Perkin-Elmer Elementar vario elemental analysis instrument. The morphology of samples was investigated by using a scanning electron microscopy (SEM Hitachi S-3500) equipped with an energy-dispersive X-ray analysis (EDX) attachment, and the accelerating voltage applied was 20 kV. The fluorescence spectra were obtained on a Shimadzu RF-5301PC fluorospectrophotometer with excitation and emission slits of 3 nm. The fluorescence decays were measured using an Edinburgh Instruments LifeSpec-ps spectrometer excited by a 372 nm laser, and the lifetimes were calculated with the F900 Edinburgh Instruments software. Photoluminescence quantum yield (PLQY) of the microbelt ensemble was measured using a HORIBA Jobin Yvon FluoroMax-4 spectrofluorimeter, equipped with an F-3018 integrating sphere. Two-photon fluorescence of the samples was excited by a 800 nm laser on a Tsunami-Spitfire-OPA-800C ultrafast optical parameter amplifier (Spectra-Physics). The fluorescence images were obtained on an Olympus U-RFLT50 fluorescence microscope.

Acknowledgements

This work was supported by the National Natural Science Foundation of China, the 973 Program (Grant no.: 2011CBA00504), 111 Project (Grant no.: B07004), Central University Research Funds and Program for Changjiang Scholars and the Innovative Research Team in University (PCSIRT: IRT1205). We gratefully acknowledge Prof. Xue Duan for the helpful discussions on this work.

Notes and references

- For examples: (a) A. C. Simonsen and H.-G. Rubahn, *Nano Lett.*, 2002, **2**, 1379; (b) X. Zhang, X. Zhang, K. Zou, C.-S. Lee and S.-T. Lee, *J. Am. Chem. Soc.*, 2007, **129**, 3527; (c) B.-K. An, S. H. Gihm, J. W. Chung, C. R. Park, S.-K. Kwon and S. Y. Park, *J. Am. Chem. Soc.*, 2009, **131**, 3950; (d) Y. Sun, K. Ye, H. Zhang, J. Zhang, L. Zhao, B. Li, G. Yang, B. Yang, Y. Wang, S.-W. Lai and C.-M. Che, *Angew. Chem., Int. Ed.*, 2006, **45**, 1825; (e) J. V. Herrikhuyzen, S. J. George, M. R. J. Vos, N. A. J. M. Sommerdijk, A. Ajayaghosh, S. C. J. Meskers and A. P. H. J. Schenning, *Angew. Chem., Int. Ed.*, 2007, **46**, 1825; (f) W. Chen, Q. Peng and Y. Li, *Adv. Mater.*, 2008, **20**, 2747; (g) Y. Lei, Q. Liao, H. Fu and J. Yao, *J. Am. Chem. Soc.*, 2010, **132**, 1743; (h) S. P. Anthony and S. M. Draper, *J. Phys. Chem. C*, 2010, **114**, 11708; (i) D. P. Yan, J. Lu, M. Wei, S. H. Qin, L. Chen, S. T. Zhang, D. G. Evans and X. Duan, *Adv. Funct. Mater.*, 2011, **21**, 2497; (j) Y. Zhao, H. Gao, Y. Fan, T. Zhou, Z. Su, Y. Liu and Y. Wang, *Adv. Mater.*, 2009, **21**, 3165; (k) J. Liang, K. Li and B. Liu, *Chem. Sci.*, 2013, **4**, 1377; (l) L. Maggini and D. Bonifazi, *Chem. Soc. Rev.*, 2012, **41**, 211; (m) N. Sary, F. Richard, C. Brochon, N. Leclerc, P. L  v  que, J.-N. Audinot, S. Berson, T. Heiser, G. Hadziioannou and R. Mezzenga, *Adv. Mater.*, 2010, **22**, 763; (n) C. A. Strassert, C.-H. Chien, M. D. G. Lopez, D. Kourkoulos, D. Hertel, K. Meerholz and L. De Cola, *Angew. Chem., Int. Ed.*, 2011, **50**, 946; (o) S. Huber and G. Calzaferri, *Angew. Chem., Int. Ed.*, 2004, **43**, 6738; (p) A. Zabala Ruiz, H. Li and G. Calzaferri, *Angew. Chem., Int. Ed.*, 2006, **45**, 5282; (q) M. Busby, H. Kerschbaumer, G. Calzaferri and L. De Cola, *Adv. Mater.*, 2008, **20**, 1614; (r) C. A. Strassert, M. Otter, R. Q. Albuquerque, A. H  ne, Y. Vida, B. Maier and L. DeCola, *Angew. Chem., Int. Ed.*, 2009, **48**, 7928.
- (a) C. Zhang, C. Zou, Y. Yan, R. Hao, F. Sun, Z. Han, Y. S. Zhao and J. N. Yao, *J. Am. Chem. Soc.*, 2011, **133**, 7276; (b) S. Tu, S. H. Kim, J. Joseph, D. A. Modarelli and J. R. Parquette, *J. Am. Chem. Soc.*, 2011, **133**, 19125.
- (a) H. Yanagi, T. Ohara and T. Morikawa, *Adv. Mater.*, 2001, **13**, 1452; (b) D. O'Carroll, I. Lieberwirth and G. Redmond, *Nat. Nanotechnol.*, 2007, **2**, 180; (c) Y. S. Zhao, H. B. Fu, A. D. Peng, Y. Ma, D. B. Xiao and J. N. Yao, *Adv. Mater.*, 2008, **20**, 2859.
- (a) L. Zang, Y. Che and J. S. Moore, *Acc. Chem. Res.*, 2008, **41**, 1596; (b) Y. Che and L. Zang, *Chem. Commun.*, 2009, 5106; (c) Z. Ning, Z. Chen, Q. Zhang, Y. Yan, S. Qian, Y. Cao and H. Tian, *Adv. Funct. Mater.*, 2007, **17**, 3799; (d) Y. Sagara and T. Kato, *Nat. Chem.*, 2009, **1**, 605.
- K. Balakrishnan, A. Datar, R. Oitker, H. Chen, J. Zuo and L. Zang, *J. Am. Chem. Soc.*, 2005, **127**, 10496.
- (a) Y. Wang, H. D. Tran, L. Liao, X. Duan and R. B. Kaner, *J. Am. Chem. Soc.*, 2010, **132**, 10365; (b) P. M. Beaujuge and J. M. J. Fr  chet, *J. Am. Chem. Soc.*, 2011, **133**, 20009; (c) A. Vidyasagar, K. Handore and K. M. Sureshan, *Angew. Chem., Int. Ed.*, 2011, **50**, 8021.
- (a) J. Hu, T. W. Odom and C. M. Lieber, *Acc. Chem. Res.*, 1999, **32**, 435; (b) Y. Xia, P. Yang, Y. Sun, Y. Wu, B. Mayers, B. Gates, Y. Yin, F. Kim and H. Yan, *Adv. Mater.*, 2003, **15**, 353.
- (a) F. J. M. Hoeben, P. Jonkheijm, E. W. Meijer and A. P. H. J. Schenning, *Chem. Rev.*, 2005, **105**, 1491; (b) D. W. P. M. L  wik, I. O. Shklyarevskiy, L. Ruizendaal, P. C. M. Christianen, J. C. Maan and J. C. M. van Hest, *Adv. Mater.*, 2007, **19**, 1191; (c) F. S. Kim, G. Ren and S. A. Jenekhe, *Chem. Mater.*, 2011, **23**, 682.
- (a) A. Patra, S. P. Anthony and T. P. Radhakrishnan, *Adv. Funct. Mater.*, 2007, **17**, 2077; (b) Z. Zhang, B. Xu, J. Su, L. Shen, Y. Xie and H. Tian, *Angew. Chem., Int. Ed.*, 2011, **50**, 11654.
- (a) J. Luo, Z. Xie, J. W. Y. Lam, L. Cheng, H. Chen, C. Qiu, H. S. Kwok, X. Zhan, Y. Liu, D. Zhu and B. Z. Tang, *Chem. Commun.*, 2001, 1740; (b) T. Qin, G. Zhou, H. Scheiber, R. E. Bauer, M. Baumgarten, C. E. Anson, E. J. W. List and K. M  llen, *Angew. Chem., Int. Ed.*, 2008, **47**, 8292; (c) Y. Hong, J. W. Y. Lam and B. Z. Tang, *Chem. Commun.*, 2009, 4332.
- (a) Z. L. Wang and J. Song, *Science*, 2006, **312**, 242; (b) F. D. Benedetto, A. Camposo, S. Pagliara, E. Mele,

- L. Persano, R. Stabile, R. Cingolani and D. Pisignano, *Nat. Nanotechnol.*, 2008, **3**, 614; (c) J. H. Kim, Y. Jung, J. W. Chung, B.-K. An and S. Y. Park, *Small*, 2009, **5**, 804; (d) C. J. Brabec, N. S. Sariciftci and J. C. Hummelen, *Adv. Funct. Mater.*, 2001, **11**, 15; (e) C. Kocher, A. Montali, P. Smith and C. Weder, *Adv. Funct. Mater.*, 2001, **11**, 31; (f) M. Yaegashi, M. Kinoshita, A. Shishido and T. Ikeda, *Adv. Mater.*, 2007, **19**, 801.
- 12 (a) Z. Fan, J. C. Ho, Z. A. Jacobson, H. Razavi and A. Javey, *Proc. Natl. Acad. Sci. U. S. A.*, 2008, **105**, 11066; (b) C. Hahn, Z. Zhang, A. Fu, C. H. Wu, Y. J. Hwang, D. J. Gargas and P. Yang, *ACS Nano*, 2011, **5**, 3970.
- 13 (a) M. Schiek, F. Balzer, K. Al-Shamery, A. Lützen and H.-G. Rubahn, *Soft Matter*, 2008, **4**, 277; (b) Y. S. Zhao, J. Wu and J. Huang, *J. Am. Chem. Soc.*, 2009, **131**, 3158.
- 14 (a) J.-M. Lehn, *Supramolecular Chemistry: Concepts and Perspectives*, VCH, New York, 1995; (b) R. V. Hameren, P. Schön, A. M. V. Buul, J. Hoogboom, S. V. Lazarenko, J. W. Gerritsen, H. Engelkamp, P. C. M. Christianen, H. A. Heus, J. C. Maan, T. Rasing, S. Speller, A. E. Rowan, J. A. A. W. Elemans and R. J. M. Nolte, *Science*, 2006, **314**, 1433; (c) A. Ajayaghosh and V. K. Praveen, *Acc. Chem. Res.*, 2007, **40**, 644.
- 15 X. Wang, J. Yan, Y. Zhou and J. Pei, *J. Am. Chem. Soc.*, 2010, **132**, 15872.
- 16 G. R. Desiraju, *Angew. Chem., Int. Ed. Engl.*, 1995, **34**, 2311.
- 17 (a) A. P. H. J. Schenning, J. Herrikhuyzen, P. Jonkheijm, Z. Chen, F. Würthner and E. W. Meijer, *J. Am. Chem. Soc.*, 2002, **124**, 10252; (b) C. R. L. P. N. Jeukens, P. Jonkheijm, F. J. P. Wijnen, J. C. Gielen, P. C. M. Christianen, A. P. H. J. Schenning, E. W. Meijer and J. C. Maan, *J. Am. Chem. Soc.*, 2005, **127**, 8280.
- 18 (a) J. Luo, T. Lei, L. Wang, Y. Ma, Y. Cao, J. Wang and J. Pei, *J. Am. Chem. Soc.*, 2009, **131**, 2076; (b) D. González-Rodríguez and A. P. H. J. Schenning, *Chem. Mater.*, 2011, **23**, 310.
- 19 (a) K. T. Holman, A. M. Pivovar and M. D. Ward, *Science*, 2001, **294**, 1907; (b) K. T. Holman, S. M. Martin, D. P. Parker and M. D. Ward, *J. Am. Chem. Soc.*, 2001, **123**, 4421; (c) B. F. Abrahams, M. G. Haywood and R. Robson, *CrystEngComm*, 2005, **7**, 629; (d) A. Soegiarto, A. Comotti and M. D. Ward, *J. Am. Chem. Soc.*, 2010, **132**, 14603.
- 20 For examples: (a) C. Löwe and C. Weder, *Adv. Mater.*, 2002, **22**, 1625; (b) J. Kunzleman, M. Kinami, B. R. Crenshaw, J. D. Protasiewicz and C. Weder, *Adv. Mater.*, 2008, **20**, 119; (c) R. E. Gill, A. Meetsma and G. Hadziioannou, *Adv. Mater.*, 1996, **8**, 212; (d) P. F. Van Hutten, V. V. Krasnikov and G. Hadziioannou, *Acc. Chem. Res.*, 1999, **32**, 257; (e) C. A. Stanier, M. J. O'Connell, W. Clegg and H. L. Anderson, *Chem. Commun.*, 2001, 493; (f) S.-J. Yoon, J. W. Chung, J. Gierschner, K. S. Kim, M.-G. Choi, D. Kim and S. Y. Park, *J. Am. Chem. Soc.*, 2010, **132**, 13675; (g) F. Gao, Q. Liao, Z. Xu, Y. Yue, Q. Wang, H. Zhang and H. Fu, *Angew. Chem., Int. Ed.*, 2010, **49**, 732; (h) H. Meier, *Angew. Chem., Int. Ed. Engl.*, 1992, **31**, 1399; (i) L. Tian, F. He, H. Zhang, H. Xu, B. Yang, C. Wang, P. Lu, M. Hanif, F. Li, Y. Ma and J. Shen, *Angew. Chem., Int. Ed.*, 2007, **46**, 3245; (j) Y. Hong, J. W. Y. Lam and B. Z. Tang, *Chem. Soc. Rev.*, 2011, **40**, 5361; (k) D. P. Yan, J. Lu, J. Ma, S. Qin, M. Wei, D. G. Evans and X. Duan, *Angew. Chem., Int. Ed.*, 2011, **50**, 7037; (l) D. P. Yan, J. Lu, J. Ma, M. Wei, D. G. Evans and X. Duan, *Angew. Chem., Int. Ed.*, 2011, **50**, 720; (m) D. Yan, A. Delori, G. O. Lloyd, T. Friščić, G. M. Day, W. Jones, J. Lu, M. Wei, D. G. Evans and X. Duan, *Angew. Chem., Int. Ed.*, 2011, **50**, 12483; (n) X. Zhou, H. Li, Z. Chi, X. Zhang, J. Zhang, B. Xu, Y. Zhang, S. Liu and J. Xu, *New J. Chem.*, 2012, **36**, 685.
- 21 J. Huang, F. Kim, A. Tao, S. Conner and P. Yang, *Nat. Mater.*, 2005, **4**, 896.
- 22 (a) K. Hirai, S. Furukawa, M. Kondo, H. Uehara, O. Sakata and S. Kitagawa, *Angew. Chem., Int. Ed.*, 2011, **50**, 8057; (b) D. Yan, G. O. Lloyd, A. Delori, W. Jones and X. Duan, *ChemPlusChem*, 2012, **77**, 1112; (c) R. G. Snyder, H. L. Strauss and C. A. Ellinger, *J. Phys. Chem.*, 1982, **86**, 5145; (d) D. Yan, J. Lu, J. Ma, M. Wei, D. G. Evans and X. Duan, *Phys. Chem. Chem. Phys.*, 2010, **12**, 15085.
- 23 M. Grell and D. D. C. Bradley, *Adv. Mater.*, 1999, **11**, 895.
- 24 B. Valeur, *Molecular Fluorescence: Principles and Applications*, Wiley-VCH Verlag GmbH, 2001.
- 25 (a) V. R. Thalladi, S. Brasselet, H.-C. Weiss, D. Blaser, A. K. Katz, H. L. Carrell, R. Boese, J. Zyss, A. Nangia and G. R. Desiraju, *J. Am. Chem. Soc.*, 1998, **120**, 2563; (b) F. Kong, S.-P. Huang, Z.-M. Sun, J.-G. Mao and W.-D. Cheng, *J. Am. Chem. Soc.*, 2006, **128**, 7750; (c) E. Cariati, Z. Yang, M. Wörle, L. Mutter, M. Jazbinsek and P. Günter, *Cryst. Growth Des.*, 2007, **7**, 83; (d) G. Cavallo, C. B. Aakeröy, N. R. Champness and C. Janiak, *CrystEngComm*, 2010, **12**, 22; (e) A. Forni, G. Leem, P. Metrangolo, F. Meyer, T. Pilati, G. Resnati, S. Righetto, G. Terraneo and E. Tordin, *Cryst. Growth Des.*, 2011, **11**, 5642; (f) C.-F. Sun, C.-L. Hu, X. Xu, B.-P. Yang and J.-G. Mao, *J. Am. Chem. Soc.*, 2011, **133**, 5561.
- 26 J. Brewer, M. Schiek, A. Lützen, K. Al-Shamery and H.-G. Rubahn, *Nano Lett.*, 2006, **6**, 2656.
- 27 Z. Hu, B. Muls, L. Gence, D. A. Serban, J. Hofkens, S. Melinte, B. Nysten, S. Demoustier-Champagne and A. M. Jonas, *Nano Lett.*, 2007, **7**, 3639.